Molecular Catalysis 480 (2020) 110650

Contents lists available at ScienceDirect

Molecular Catalysis

journal homepage: www.elsevier.com/locate/mcat

CuO grafted triazine functionalized covalent organic framework as an efficient catalyst for C-C homo coupling reaction

Sabuj Kanti Das[a], Bijan Krishna Chandra[a,b,1], Rostam A. Molla[c,1], Manideepa Sengupta[c], Sk. Manirul Islam[c], Adinath Majee[b], Asim Bhaumik[a,*]

[a] School of Materials Sciences, Indian Association for the Cultivation of Science, 2A & B Raja S. C. Mullick Road, Jadavpur, Kolkata, 700032, India
[b] Department of Chemistry Visva-Bharati University, Shantiniketan, 731235, India
[c] Department of Chemistry Kalyani University, Kalyani, 741235, India

ARTICLE INFO

Keywords:
Covalent organic framework
Heterogeneous catalysis
CuO nanoparticles
Immobilization of metal oxides over porous nanomaterials
C-C homo coupling reaction

ABSTRACT

Designing of low cost catalytic system for new C-C bond formation reactions is very challenging in synthetic organic chemistry. Herein, we report a new copper oxide immobilized covalent organic framework (COF) material Cu^{II}-TRIPTA by grafting of CuO nanoparticles at the surface of a nitrogen rich porous COF material TRIPTA. TRIPTA has been synthesized through the extended Schiff base reaction between 2,4,6-triformylphloroglucinol and 1,3,5-tris-(4-aminophenyl) triazine. The COF as well as CuO loaded materials are characterized by powder X-ray diffraction (PXRD), transmission electron microscopy (TEM), X-ray photoelectron spectroscopy (XPS), N_2 adsorption-desorption, Fourier transform infrared spectroscopy (FT-IR), thermogravimetry (TG) and EPR spectroscopic analyses. Cu^{II}-TRIPTA material has been successfully applied as heterogeneous nanocatalyst for the C-C homo-coupling reaction of phenylboronic acids to synthesise wide range of biaryl compounds under mild and eco-friendly conditions (60 °C, methanol solvent). Remarkably high specific surface area of Cu^{II}-TRIPTA (583 m^2 g^{-1}) and highly accessible catalytic sites in the 2D-hexagonal COF nanoarchitecture potentially makes it excellent catalyst in the C-C bond formation reaction, which is evident from the high TON of the catalyst in this reaction. The catalyst was recollected and reused till 6^{th} cycles without any noticeable change of its catalytic activity, suggesting its high catalytic efficiency in this C-C bond formation reaction.

Introduction

COFs possessing two to three dimensional crystalline polymeric structures with stable nano scale porosity [1,2] are formed by covalent linking via extended polymerization reaction between various reactive organic monomers. These materials are largely utilized in the recent times for different promising applications of energy and environmental research, like gas storage [3,4], gas separation [5], sensing [6], metal ion adsorption [7], light emitter [8], heterogeneous catalysis [9–11], photocatalysis [12], and so on. Like COFs a wide diversity of organic porous materials viz. porous organic polymer (POPs) [13], conjugated microporous polymers (CMPs) [14], covalent triazine frameworks (CTFs) [15] can also be constructed via extended polymerization between the multipodal monomeric building units. Due to large surface area, physicochemical stability together with pores of nanoscale dimensions, these porous nanomaterials are often employed to support for designing suitable heterogeneous catalysts [16] to synthesise valued fine chemicals. The surface of these COFs can offer wide opportunity for the grafting of different transition and non-transition metal/metal oxide nanoparticles [17,18], which could facilitate the easy diffusion of organic reactants and products from the active sites of the catalysts [19–22].

C-C bond formation reactions are very demanding in synthetic organic chemistry; especially in the context of designing biologically active compounds and reactive organic functionalities having a broad spectrum of applications [23–27]. They are also utilized for the synthesis of various mono to polydentate ligands [28], which can be further used for synthesizing different organic and organic-inorganic hybrid materials [29,30]. Generally Pd, Ru based catalysts are intensively studied for the synthesis of different organic moieties through C-C homo and cross-coupling reactions [30,31]. Bhunia et al. have analyzed Pd grafted nitrogen rich organic porous framework as a robust

* Corresponding author.
E-mail address: msab@iacs.res.in (A. Bhaumik).
[1] These authors contribute equally.

https://doi.org/10.1016/j.mcat.2019.110650
Received 24 June 2019; Received in revised form 28 September 2019; Accepted 30 September 2019

support for carrying out the C-C cross coupling reaction [30]. Alonso et al. have described the Pd catalysed heterogeneous homocoupling of terminal alkynes [32]. Venkatraman et al. have shown C-C coupling reaction in homogeneous phase using Pd as catalyst in air and water [33]. A large number of C-C homo coupling reactions are reported using Pd as catalyst and many reactions have been performed homogeneously [34,35]. But the major disadvantage of these reactions includes use of toxic reagents, hazardous solvents as well as expensive metal and ligand sources. Thus, novel approach to achieve efficient C-C coupling reaction using inexpensive catalytic system is highly desirable. So low cost and abundant metal like Cu, Fe, Ni, Ag based catalysts have attracted overwhelming attention in C-C coupling reactions in the recent times [36–39].

In this context Liu et al. reported homo coupling reactions of aryl Grignard reagents in presence of O_2 with Fe as catalyst for the formation of new C-C bond [40]. Xiao et al. have shown homo coupling reaction proceeds smoothly over the Mg-Al oxide stabilized gold nanoparticles [41]. Sakurai et al. studied the homo coupling reaction of arylboronic acids employing gold nanoparticles as catalyst in acidic medium [42]. Indium was also employed for reductive homo coupling between alkyl and aryl halides by Ranu et al. [43]. Zn containing catalyst and Pd grafted Zn based MOF have been reported for C-C coupling reaction by G. Anilkumar et al. and M. Azad et al. respectively [44,45]. Very recently Yongjun Liu et al. reported copper-catalysed C-C homocoupling of alkyl halides in the presence of another metal samarium [46]. But most of the reactions are associated with inherent drawbacks of toxicity, noneconomical, hazardous organic solvents, which are not acceptable in the context of bulk scale synthesis following green chemistry protocol. Among the various transition metal, 3d series metal Cu is considered for catalyst due to its low toxic nature and higher stability. Cheng et al. showed homogeneous catalysis of C-C homo coupling reaction by $CuCl_2$ [47]. Alonso et al. reported a Cu(II) catalysed heterogeneous homo coupling of terminal alkyne in their different oxidation state [32]. Yaghi et al. and Puthiaraj et al. reported homo coupling reactions of arylboronic acids using/without using external base where Cu based MOFs, $Cu_3(BTC)_2$ [48] and Cu(BDC) [49] are used as catalyst.So C-C homo coupling reaction catalyzed by Cu(II) supported nanoporous materials with high surface area is very challenging.

Herein, we have synthesized a nitrogen and phenolic − OH rich COF material TRIPTA through solvothermal Schiff base condensation of 2,4,6-triformylphloroglucinol and 1,3,5-tris-(4-aminophenyl)triazine in a pressure tube and further decorated its surface with CuO nanoparticles to yield an efficient heterogeneous catalyst Cu^{II}-TRIPTA (Scheme 1). Then we have explored the catalytic activity of Cu^{II}-TRIPTA in the C-C homo coupling reaction of aryl boronic acids for the synthesis of biaryl derivatives.

Experimental section

Chemicals

1,3,5-triformyl phloroglucinol (TFP), was synthesised from phloroglucinol (Sigma-Aldrich, India). Hexamine, trifluoroacetic acid and hydrochloric acid were obtained from Merck, India.1,3,5-tris-(4-aminophenyl) triazine (TAPT), was synthesised from 4-aminobenzonitrile and trifluoromethanesulfonic acid which were obtained from Sigma-Aldrich, India. Anhydrous N,*N*-dimethylformamide, copper salts CuCl, $CuCl_2$ and $Cu(OAc)_2$ and all substrate used for the catalytic study were obtained from Spectrochem, India; all are used without further purification. All other solvents used were of analytical grade produced by Merck, India and were distilled prior to use.

Material characterizations

Powder X-ray diffraction study of both the TRIPTA and Cu^{II}-TRIPTA COFs were done in a Bruker AXS D-8 Advanced SWAX diffractometer using *Cu-K* α (λ = 0.15406 nm) radiation. Diffraction patterns in the wide angle region (10° − 80°) were recorded at a rate of (2θ) = 0.4° per min and that of small angle region (2°-10°) were recorded at a rate of (2θ) = 0.2° per min. Ultra high resolution transmission electron microscopic (TEM) images of the COF and subsequent CuO loaded COF, were taken by using a UHR-FEG TEM system (JEOL JEM 2100 F) transmission electron microscope operating at 200 kV electron source. Samples were prepared by dropping a sonicated ethanolic dilute solution of the COF TRIPTA and Cu^{II}-TRIPTA materials over a carbon coated copper grid followed by drying under high vacuum. N_2 adsorption/desorption isotherm of both the materials were obtained froma Autosorb-iQ surface area analyzer of Quantachrome Instruments, USA at 77 K to calculate the Brunauer-Emmett-Teller(BET) surface area as well as material porosity. Pore size distribution plot was obtained by usingnon local density functional theory (NLDFT) taking N_2 sorption at 77 K on carbon with slit pore model as reference. Prior to the sorption measurement, the powder sample was Sohxlet extracted for 72 h usinganhydrous MeOH as dispersion medium and dried itunder vacuum at 150 °C. Prior to all the adsorption study, both the samples were degassed at 423 K for 12 h under high vacuum conditions. Thermogravimetric analysis (TGA) was performed using a Mettler Toledo TGA/DTA 851e TA-SDT Q-600 instruments. The EPR (electron paramagnetic resonance) spectroscopic analysis has been done for both the freshly synthesized catalyst as well as used catalyst at room temperature using a JES-FA200ESR spectrometer (JEOL). FTIR study of boththe TRIPTA and Cu^{II}-TRIPTA were recorded from Perkin Elmer Spectrum 100 spectrophotometer.

Synthesis of COF TRIPTA

We have carried out the Schiff base condensation between TFP and TAPT for the synthesis of this TRIPTA COF in a Pyrex sealed tube [50]. Within an oven dried clean Pyrex sealed tube we have mixed 0.4 mmol TAPT (141.2 mg) and 0.4 mmol TFP (84 mg) in 1:1 M ratio. In that 3 mL dioxane, 3 mL mesitylene, and 0.5 mL CH_3COOH 6(N) were added. Then the reaction mixture was sonicated for 20 min to make homogeneous mixture and followed by degassing three times with the freeze-pump-thaw cycle using liquid N_2 and high vacuum pump. Then the Pyrex tube was flame sealed and allows this solvothermal reaction to proceed for 4 days. Finally the deep **orange-red** colou**red** fine powder material filte**red** off and washed with ethanol followed by THF to remove unreacted starting monomers. Then the guest free porous material was obtained by Soxhlet extraction with THF: methanol (1:1) for 48 h and dried under vacuum at 150 °C for overnight. The isolated yield of the COF material was obtained 81 wt%.

Synthesis of Cu^{II}-TRIPTA catalyst

To an methanolic solution of the TRIPTA (0.5 g material with 50 ml of MeOH) 0.2(M) 25 mL of $CuCl_2$ solution was added and allowed to stir for overnight at room temperature in open air condition. The resultant slurry was washed successively with water to wash out inorganic residue if any, then with acetone and ethanol. Then the resultant solid was air dried for 2 days. Then the material was characterized thoroughly and after getting satisfactory characterization results its catalytic activity was explored.

General procedure for homo coupling reaction catalyzed by Cu^{II}-TRIPTA:

Biaryl derivatives were synthesized from phenylboronic acids in methanol solvent. In a typical experiment 1 mmol of phenylboronic acid was taken in 5 mL methanol and then 30 mg of Cu^{II}-TRIPTA catalyst was taken into the reaction mixture. The reaction was proceeded for 5–12 h at 60 °C temperature under air. After completion of the coupling reaction, the reaction mixture was allowed to cool at room temperature and water and ethyl acetate was added to it. Further using a separating funnel organic layer was collected 4 times and dried to

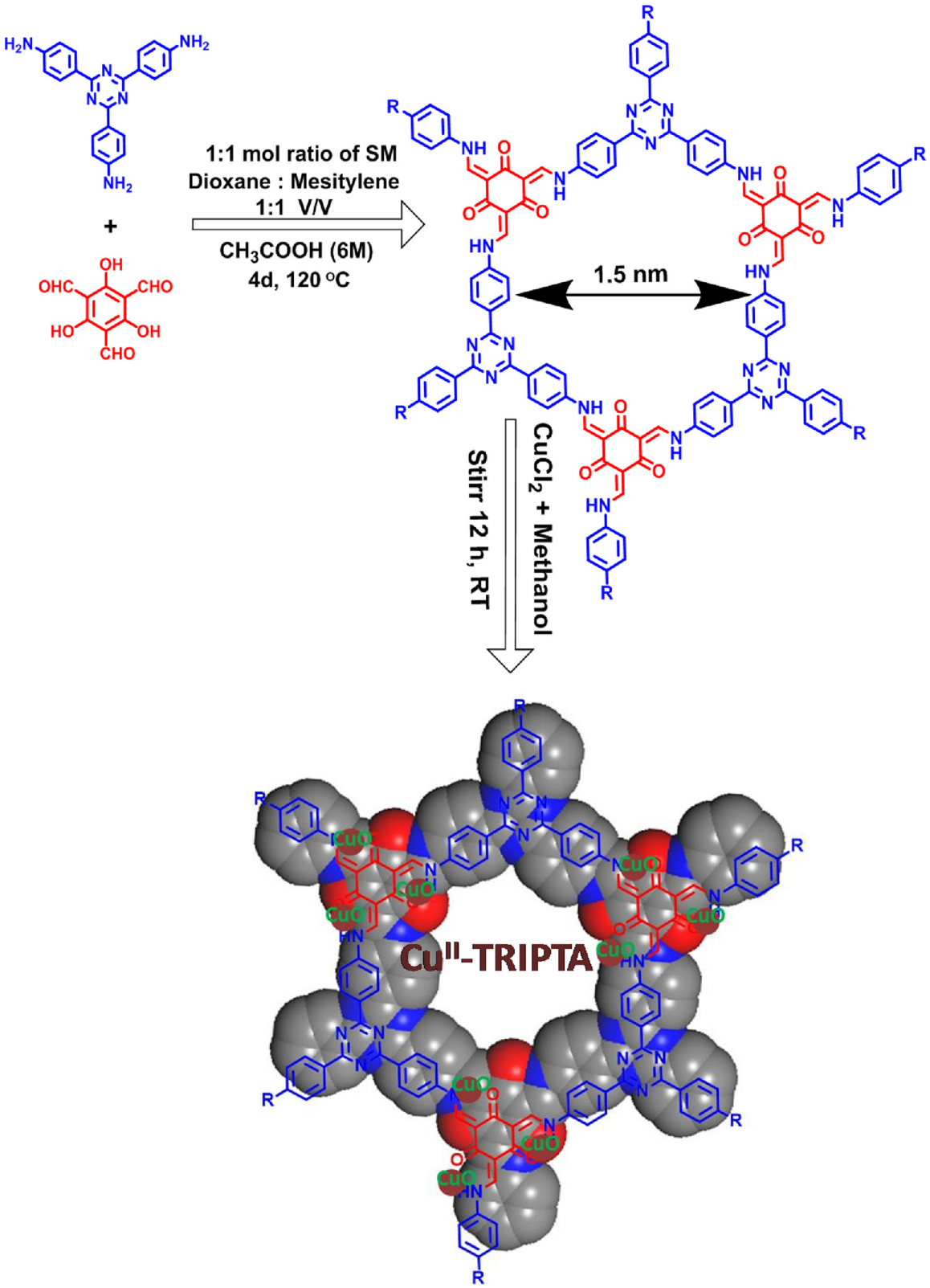

Scheme 1. Synthetic pathway for designing Cu^{II}-TRIPTA.

obtain pure biphenyl derivatives. All the isolated desired products were characterized by taking ^{1}H NMR.

Results and discussion

As seen in Scheme 1, that a 2D hexagonal COF can be constructed through simple Schiff base condensation reaction between the triarmed amine and aldehyde, which is further decorated with CuO nanoparticles at its surface for the synthesis of Cu^{II}-TRIPTA material. Cu^{II}-TRIPTA has been utilized as a heterogeneous catalyst for C-C homo coupling reaction (Scheme 2).

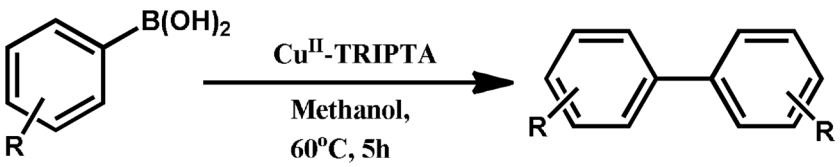

Scheme 2. Heterogeneous Cu^{II}-TRIPTA catalyzed C-C homo coupling reaction of arylboronic acids.

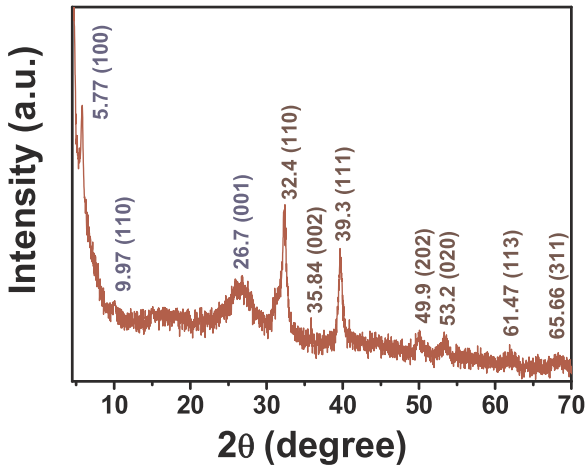

Fig. 1. PXRD analysis of Cu^{II}-TRIPTA material.

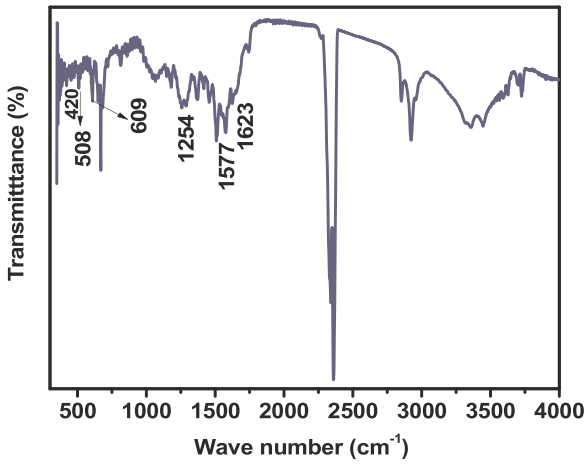

Fig. 2. FTIR spectrum of Cu^{II}-TRIPTA.

X-ray diffraction studies

Powder X-ray diffraction spectra of Cu^{II}-TRIPTA is shown in Fig. 1. The PXRD pattern of the pristine TRIPTA COF material is also shown in Figure-S1,which displayed similar peaks at 2 θ = 5.6, 9.8, 15.3 and 26.4° [6] corresponding to the hexagonally arranged pores with the respective crystal planes 100, 110, 210 and 001. The diffraction pattern as shown in Fig. 1 is in complete agreement with identical structural feature of the material having 2D sheet like crystalline periodic hexagonal framework. The diffraction hump located at about 2θ = 26.2° can be explained due to the presence of $\pi - \pi$ stacking between the 2D sheets of the ordered hexagonal phase and was designated as (001) reflection plane. On the other hand, the powder diffraction pattern of Cu^{II}-TRIPTA displayed additional peaks at 2θ = 32.44, 35.84, 39.33, 49.95, 53.26, 61.47 and 65.66° of 2θ (Fig. 1). These could be attributed to the (110), (002), (111), (202), (020), (113), and (311), faces of the monoclinic crystalline CuO NPs [51,52] stuck at the surface of the COF (TRIPTA). Further, very little shifts in the peaks of the COF, which appeared at 5.77, 9.97 and 26.7, corresponding to the 100, 110, 001, planes of TRIPTA suggested successful loading of CuO nanoparticle at the surface of the COF. Thus, copper oxide nanoparticles are grafted through the reaction between TRIPTA COF and $CuCl_2$.

FT-IR spectroscopy

FTIR spectra of TRIPTA (Fig. S2) and Cu^{II}-TRIPTA (Fig. 2) materials suggested the formation of desired bonding and connectivity. FTIR spectrum of Cu^{II}-TRIPTA showed all characteristics peaks of this COF such as 1620 cm^{-1} for carbonyl group [−C=O], 1576 cm^{-1} for [−C=C−], 1255 cm^{-1} for [−C=N−] stretching vibrations, which suggested the formation of TRIPTA through the Schiff base polycondensation reaction [6]. Along with those peaks some new peaks are appeared at 420, 508 &610 cm^{-1}, which could be assigned due to the stretching vibration of Cu-O bond of CuO, confirming the presence of CuO nanoparticles bound in the COF polymer network [51,52]. No peak appeared at 1615 cm^{-1}, which suggested the absence of Cu-O stretching vibration of Cu_2O. As a result FTIR analysis indicates the successful binding of CuO NPs in the Cu^{II}-TRIPTA material.

N_2 adsorption-desorption

N_2 sorption analysis has been carried out to understand the porosity and surface areas of TRIPTA and Cu^{II}-TRIPTA materials. Corresponding isotherms are shown in Fig. 3a and b. N_2 adsorption/desorption isotherms of TRIPTA can be classified as type I corresponding to large micropores, whereas that for Cu^{II}-TRIPTA displayed features of type I together with a steady uptake of N_2 in the intermediate region of P/P_0 corresponding to the presence of broad range of mesopores [53]. Loading of CuO NPs in the TRIPTA COF may create additional interparticle voids, which could be the origin of mesoporosity in Cu^{II}-TRIPTA material [54]. Calculated BET surface areas of TRIPTA and Cu^{II}-TRIPTA materials are 1014 and 583 $m^2\,g^{-1}$, respectively. Implying NLDFT theorem, and using the N_2 adsorption desorption isotherm pore size distribution plots has been calculated which clearly indicates the peak pore widths are 1.54 and 1.75 nm for TRIPTA and that of Cu^{II}-TRIPTA is 1.21, 1.54 nm. Respective pore volumes of these two materials were 1.91 and 0.93 $cm^3\,g^{-1}$, respectively. So further lowering all thesein surface area, pore size and pore volume in the CuO loaded COF suggested there is a successful decoration of CuO nanoparticles at the surface of the TRIPTA COF material in Cu^{II}-TRIPTA.

Morphological analysis

Ultra high resolution transmission electron microscopic (UHR-TEM) images of the as-synthesized and recycled Cu^{II}-TRIPTA materials after the catalytic reactions are shown in Fig. 4a–d respectively. As seen from these images that spherical CuO nanoparticles are uniformly distributed in TRIPTA COF corresponding to the dark spots throughout the specimen grid in Cu^{II}-TRIPTA (Fig. 4a and b). This result suggested the successful binding of CuO nanoparticles in the polymer framework. These images further revealed homogeneous distribution of the CuO NPs over the COF support with an average particle size of 6.58 nm [55,56]. TEM images of recycled catalyst Cu^{II}-TRIPTA (Fig. 4c and d) clearly indicates the retention of structural morphology of catalyst after six consecutive reaction cycles.

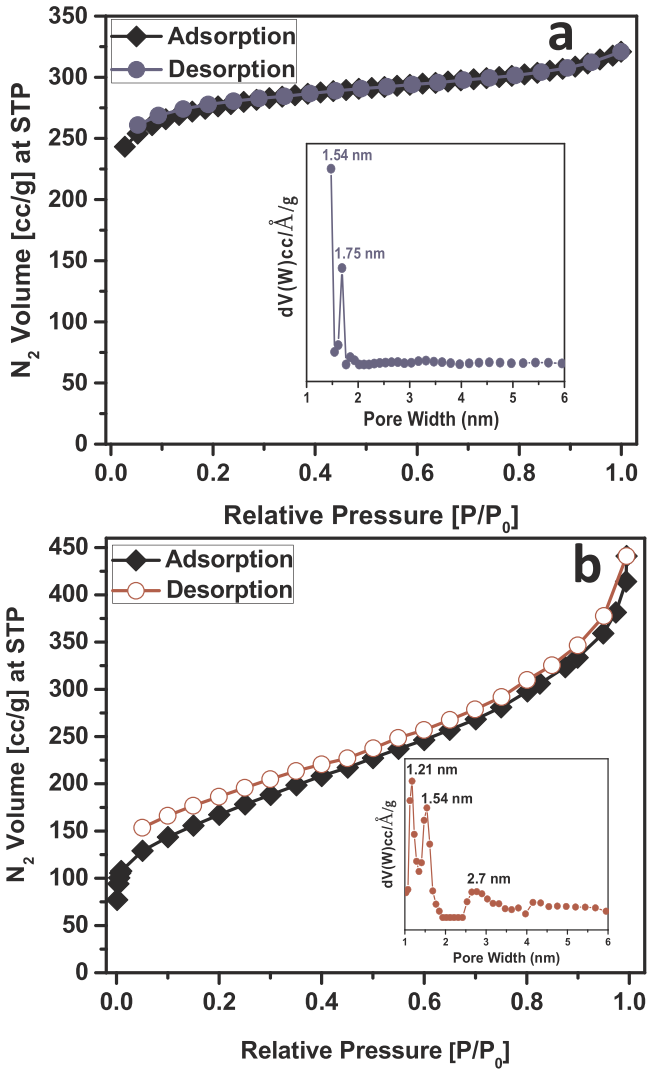

Fig. 3. N_2 sorption isotherms of TRIPTA (a) and Cu^{II}-TRIPTA (b). Respective pore size plots are shown in the insets.

Thermogravimetric analysis

Thermogravimetric analysis (TGA) of the TRIPTA and Cu^{II}-TRIPTA has been carried out in abroad span oftemperaturefrom 35 to 800 °C with a temperature ramp of 10 °C min^{-1} under N_2 flow (Figure S3). From the TGA curve of TRIPTA, we found that it is thermally stable upto 390 °C. Further, the TGA plot of Cu^{II}-TRIPTA dictates first weight loss below 100 °C which is due to the fact of evaporation of water absorbed in the surface of the catalyst. After that a significant decrease in the weight is observed beyond 280 °C, which revealed that Cu^{II}-TRIPTA framework is stable up to 280 °C. These results, our catalyst is highly stable upto a large temperature span(upto 280 °C), where the liquid phase catalytic reactions are usually carried out and covered.

Electron paramagnetic resonance spectroscopy

Oxidation state of CuO loaded catalyst was confirmed from EFR spectroscopic analysis. The EPR study has been conducted for Cu^{II}-TRIPTA material before and after the catalytic reactions (Fig. 5). We found that the sample is EPR active and a characteristic singlet absorption peak observed in Cu^{II}-TRIPTA (Fig. 5) suggested that mostly +2 oxidation state of Cu is present in this material. This pattern also revealed an anisotropic spectrum having signals of the axial or orthorhombic type geometry of the Cu indicating elongation along the z axis [57]. The similar spectral features of the catalyst before and after the catalytic study indicates unchanged oxidation state of copper (Cu^{+2}) for both the fresh and reused catalysts under aerial exposer. To examine the change in the oxidation state of copper during the reaction pathway we have collected the catalyst at an intermediate time of the reaction and after completion of the reaction under inert atmosphere. Two separate EPR spectra were studied to compare the difference among them, as well as with the pristine COF (ESI S-12 a,b). This contrast study indicates little changes of spectral pattern, which is due to mixed valance state of Cu species (Cu^{I}/Cu^{II}) within the catalytic system [58,59]. Change in the shape of Cu(II) spectrum could be attributed to the superposition of two kinds of signals (due to the presence of original Cu(II) and that of newly formed Cu(II) species under inert atmosphere).

X-ray photoelectron spectroscopy (XPS)

The XPS spectra of O 1s and Cu 2p in Cu^{II}-TRIPTA catalyst are shown in Fig. 6a and b. From the XPS study we found two peaks for O 1s at binding energies 529 and 531 eV (Fig. 6a) [55], which could be attributed to the O 1s of CuO nanoparticle and the O present in the organic framework. For Cu 2p also we find twobinding energy values 933.9 and 953.7 eV (Fig. 6b), which can be attributed to thespin orbit splitting components Cu $2p_{3/2}$ and Cu $2p_{1/2}$ of copper and this is in good agreement with the reported binding energies of Cu(II) [60]. The distinctive 2p to 3d satellite peak for Cu in +2 oxidation state was also present in this XPS spectrum. So from this XPS analysis we can conclude the Cu species in the Cu^{II}-TRIPTA is in the +2 oxidation state. Full scale XPS of Cu^{II}-TRIPTA for all elements present in the catalyst is shown in the (Figure S4), suggesting the presence of other elements C and N in this supported COF material. We have used this XPS analysis data to evaluate the atomic percentages of different elements present in the supported COF material, which suggested the presence of C = 58.44%, N = 11.07%, O = 29.50%, Cu = 0.99%.

Catalysis

Cu^{II}-TRIPTA catalysed C-C homo coupling reaction:

C-C homo coupling and optimisation of reaction conditions:

To check the efficiency of this heterogeneous Cu^{II}-TRIPTA catalyst, we have performed the C-C homo coupling reactions of arylboronic acids to get biaryl derivatives. Although there are several homogeneous copper catalysts reported for this reaction, heterogeneous copper catalysts still have a wide scope if the catalyst is chemically robust, reusable and less time consuming. Initially biphenyl was synthesized via C-C homo coupling of phenylboronic acid over Cu^{II}-TRIPTA. Phenylboronic acid (1 mmol), Cu^{II}-TRIPTA catalyst (30 mg) and methanol (5 ml) was taken initially to carry out the reaction at 40 °C temperature in open air. Outcome of this experiment suggested that the catalyst is highly reactive in this reaction. Under this reaction condition yield of the biphenyl was 83%. To optimize the reaction conditions we have screened several reaction parameters and these are listed in Table-1.

To optimize the reaction parameters then we have screened the yield of this reaction with different solvents. Various protic and aprotic solvents were tested. Table1 revealed alcoholic solvents are more effective for this C-C coupling reaction. Among them methanol was most effective. On the other hand, polar or non-polar aprotic solvents were not effective in the reaction. Alcoholic solvents are highly polar and also can act as reducing agent to facilitate the reaction. Interestingly even under mild reaction conditions, i.e. at 40 °C temperature this C-C coupling reaction could give excellent yields. When temperature was raised to 60 °C in methanol solvent, a further 13% yield was increased. Even at 80^0 C temperature yield remain same as that of 60 °C. So, 60 °C temperature was taken as an optimum temperature for this C-C coupling reaction under open air condition.

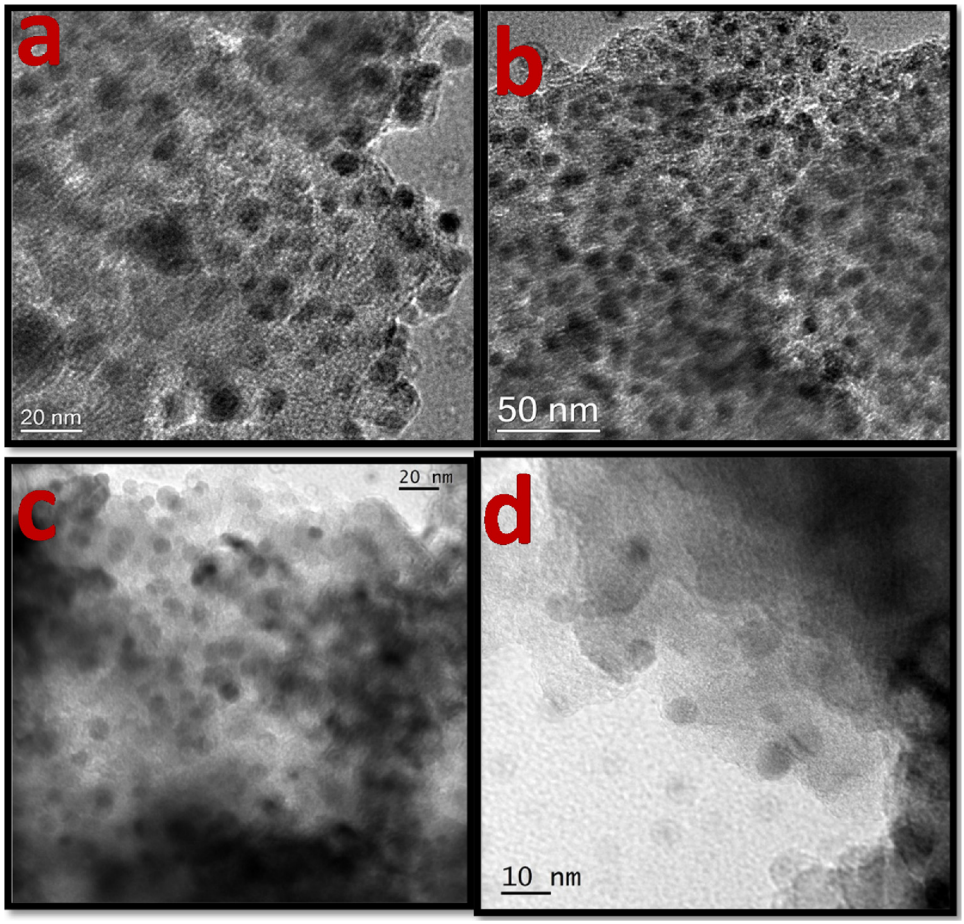

Fig. 4. TEM images of as-synthesized Cu^{II}-TRIPTA material (a, b) and recycled Cu^{II}-TRIPTA material (c, d).

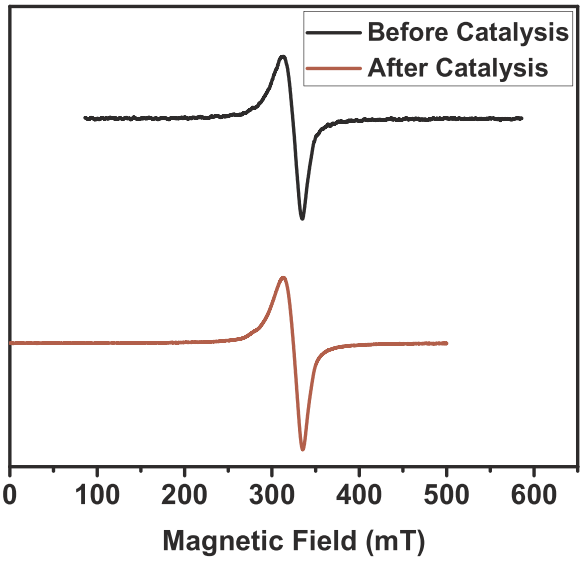

Fig. 5. EPR spectra of fresh (black) and reused (red) Cu^{II}-TRIPTA catalyst.

Reaction conditions: phenylboronic acid (1 mmol), solvent (5 ml), catalyst (30 mg), reaction time (5 h) in open air condition.

Copper catalyst plays crucial role in this reaction because without catalyst this reaction could not proceed. Other copper salts such as $CuCl_2$, CuCl and $Cu(OAc)_2$ also effective for this type of reaction but homogeneous salts are not easily separable from the reaction mixture, which made the product recovery and recycling highly unfeasible. Further, it is pertinent to mention that, only small amount of Cu^{II}-TRIPTA

Reaction conditions: phenylboronic acid (1 mmol), MeOH (5 ml), catalyst (30 mg), reaction temperature = 60 °C in open air condition.

Catalyst was enough for carrying out this reaction. Due to large surface area of the catalyst Cu^{II}-TRIPTA, the reaction can easily carried out at the surface of this supported catalyst. Reaction time is also crucial for this reaction and maximum yield was obtained after 5 h. Details of this C-C homo coupling reaction over different catalytic systems are summarized in Table 2. After completion of optimization of the reaction conditions several arylboronic acids were used as substrate to obtain their corresponding biaryl derivatives. Table 3 showed respective yields of the homo coupling reaction products on various arylboronic acids. As seen from this table that in every case good to excellent yields were obtained and it is seen that the reactions proceed smoothly for either electron donating or withdrawing substituent present in the arylboronic acids. Most of the cases electron donating group containing para substituted arylboronic acids was able to produce slightly higher yield than electron withdrawing groups. Under the optimum condition for different arylboronic acids 59% to 96% of isolatedyields of the biaryl products are obtained together with moderately good turn over numbers (TONs = 28 to 45, Table 3). The loading of Cu estimated in Cu^{II}-TRIPTA(0.99 mol% from XPS) was used for TON calculation (Supporting information, Section S2).

Reaction conditions: Boronic acid (1 mmol), MeOH (5 ml), catalyst (30 mg), reaction Temp. (60 °C), time (5 h), isolated yield was determined by ^1H NMR (supporting information, Figure S5-S11) in open air condition.

A plausible mechanism for this C-C coupling reaction is shown in Figure S13. In the presence of MeOH and triazine moiety of the TRIPTA

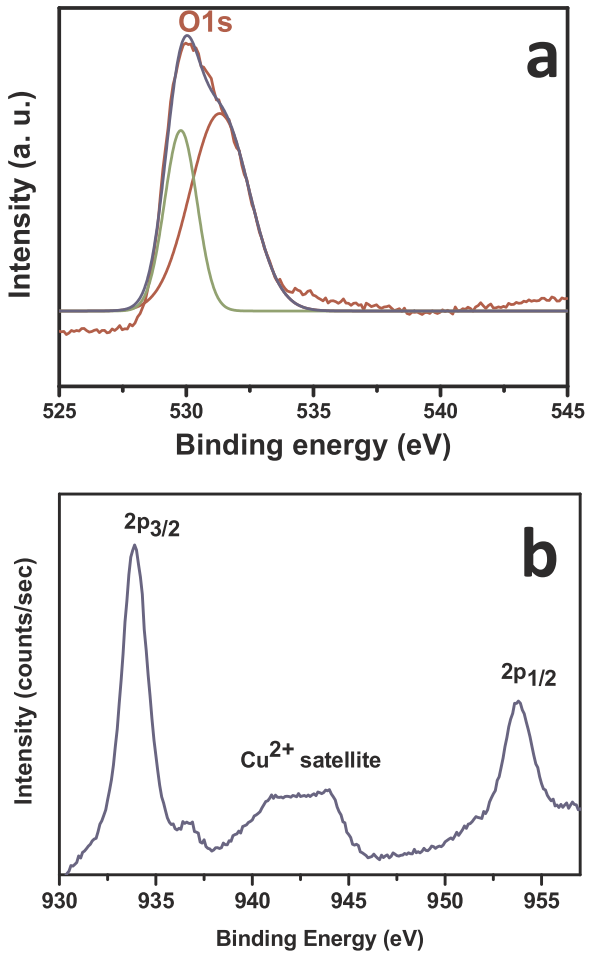

Fig. 6. XPS spectrum of Cu^{II}-TRIPTA catalyst: O1 s (a) and Cu2p (b). (For interpretation of the references to colour in this figure legend, the reader is referred to the web version of this article).

Table 1
Effect of solvent and temperature on the reaction.

Entry	Solvent	Temp.(°C)	Yield (%)
1	Methanol	40	83
2	Methanol	60	96
3	Ethanol	60	92
4	iPrOH	60	88
5	Toluene	60	Trace
6	DMF	60	Trace
7	Methanol	80	96

Table 2
: Effect of catalyst and reaction time on the reaction.

Entry	Catalyst	Reaction time (h)	Yield (%)
1	Cu^{II}TRIPTA	5	96
2	Cu^{II}TRIPTA	4	84
3	Cu^{II}TRIPTA	3	64
4	Cu^{II}TRIPTA	6	96
5	$CuCl_2$	6	83
6	$Cu(OAc)_2$	6	72
7	CuCl	6	93
8	–	6	0

COF, Cu^{II} may be reduced to Cu^{I} which then undergoes transmetallation, oxidative addition followed by reductive elimination via Cu(I)/Cu (III) intermediates [61]. Finally after the catalytic reaction cycle under aerobic conditions Cu(I) oxidised to Cu^{II} [62,63].

Table 3
C-C homo coupling of different substrates for the synthesis of biaryl derivatives catalyzed by Cu^{II}-TRIPTA.

Entry	-R	Product	Yield(%)	TON
1	Ph	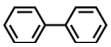	96	45
2	4-CH_3-Ph	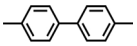	94	44
3	4-OCH_3-Ph	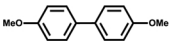	91	43
4	4-CH_2O-Ph	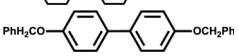	84	39
5	4-Cl-Ph	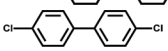	89	42
6	3-F-Ph	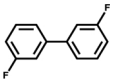	92	43
7	2-OH-Ph	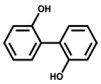	68	32
8	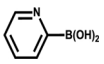	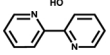	59	28

Recycling test

For any heterogeneous catalyst recyclability is the most important aspect, where its potentiality for easy separation from the reaction mixture, recoverability and reusability are taken into consideration. The reusability of the Cu^{II}-TRIPTA catalyst was studied in the representative C-C homo coupling reaction of phenylboronic acid and 4-chlorophenylboronic acid under the optimized reaction conditions separately (Table 3, entry 1 and 5). After first cycle of the reaction, the catalyst was collected by simple filtration through a sintered glass-bed (G-4) and washed with ethanol then with acetone. Then the catalyst was oven dried at 100 °C or by simple air dried for 2 days. Up to six successive runs the performance of the recycled catalyst for the targeted reaction was tested for 5 h reaction time and the corresponding product yields are shown in Fig. 7. This plot indicated that the catalytic activity of the recovered catalyst decreased from 96% to 87% for phenylboronic acid and 89% to 80% for 4-chlorophenylboronic acid respectively after

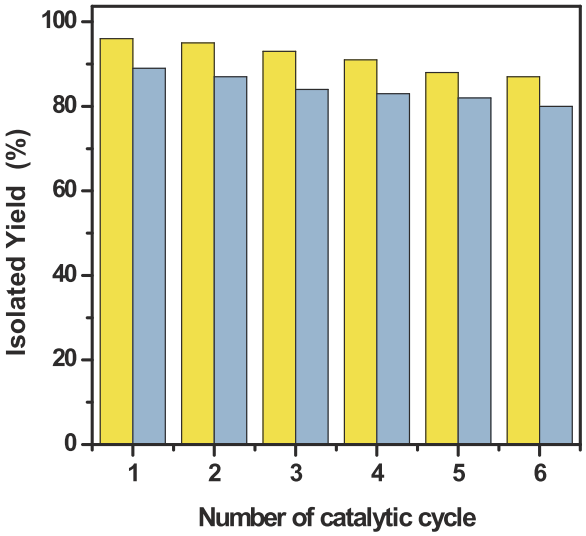

Fig. 7. Recycling efficiency of Cu^{II}-TRIPTA catalyst in the C-C homo coupling reaction of phenylboronic acid (yellow) and 4-chlorophenylboronic acid (cyan). (For interpretation of the references to colour in this figure legend, the reader is referred to the web version of this article).

six consecutive reaction cycles. This result suggested considerably good recycling efficiency of Cu^{II}-TRIPTA in this C-C homo coupling reaction.

Heterogeneity test

A controlled leaching experiment was carried outin this C-C homo coupling reaction of phenylboronic acid (Table 3, entry 1) over Cu^{II}-TRIPTA catalyst so as to examine any trace amount of copper being leached out from the catalystto the solution. Among the various proofs of heterogeneity, a simple and convenient test filtration (separation of catalyst at the middle of the reaction) was carried out. Here we have separated the catalyst after 3 h advancement of the reaction by simple filtration from the reaction mixture and the filtrate i.e., the reaction mixture was allowed to react up to 5 h i.e., till its completion time. No further reaction advancement was noticed, which revealed the catalyst is perfectly heterogeneous by performance. In addition to that there was no evidence of decomposition of the solid catalyst during the entire catalytic reaction. In addition to that the supernatant of the reaction mixture as collected by simple filtration, was further examined through atomic absorption spectroscopy, which suggested the absence of Cu(II) in the liquid phase. This result suggested no leaching Cu(II) species from the catalyst surface occurred to the reaction medium during the entire course of the reaction.

Conclusions

Our experimental results suggested that CuO nanoparticles can be grafted at the surface of COF material having high specific surface area and resulting material can be utilized as a heterogeneous catalyst for C-C homo coupling reaction to produce different type of biaryl compounds from respective phenylboronic acids without using any external base. The catalyst provides several advantages in this C-C coupling reaction; such as convenient and mild reaction conditions, ligand-free protocol, use of trace copper content (0.99 atom % by XPS), reaction in MeOH (cheap solvent), high yields (59–96%) of products, long range recyclability along with negligible loss in activity. Such a green C-C coupling reaction of different arylboronic acids over efficient and highly recyclable copper oxide nanoparticle grafted COF catalyst reported herein, have huge potential for the synthesis of value added biaryl compounds via C-C homo coupling reaction in future.

Acknowledgements

SKD wishes to thank UGC, New Delhi for senior research fellowship. BKC wishes to thank IACS and Visva-Bharati University, Shantiniketan for infrastructural research support. AB wishes to thank DST, New Delhi for DST-SERB core research grant.

Appendix A. Supplementary data

Supplementary material related to this article can be found, in the online version, at doi:https://doi.org/10.1016/j.mcat.2019.110650.

References

[1] X. Feng, X. Ding, D. Jiang, Chem. Soc. Rev. 41 (2012) 6010–6022.
[2] Q. Sun, B. Aguila, L.D. Earl, C.W. Abney, L. Wojtas, P.K. Thallapally, S.Q. Ma, Adv. Mater. 30 (2018) 1705479(1-9).
[3] H. Furukawa, O.M. Yaghi, J. Am. Chem. Soc. 131 (2009) 8875–8883.
[4] R. Gomes, P. Bhanja, A. Bhaumik, Chem. Commun. 51 (2015) 10050–10053.
[5] B.P. Biswal, H.D. Chaudhari, R. Banerjee, U.K. Kharul, Chem. Eur. J. 22 (2016) 4695–4699.
[6] R. Gomes, A. Bhaumik, RSC Adv. 6 (2016) 28047–28054.
[7] Q.Y. Lu, Y.C. Ma, H. Li, X.Y. Guan, Y. Yusran, M. Xue, Q.R. Fang, Y.S. Yan, S.L. Qiu, V. Valtchev, Angew. Chem. Int. Ed. 57 (2018) 6042–6048.
[8] S. Dalapati, S. Jin, J. Gao, Y. Xu, A. Nagai, D. Jiang, J. Am. Chem. Soc. 135 (2013) 17310–17313.
[9] Y.W. Peng, Z.G. Hu, Y.J. Gao, D.Q. Yuan, Z.X. Kang, Y.H. Qian, N. Yan, D. Zhao, ChemSusChem 8 (2015) 3208–3212.
[10] P. Puthiaraj, W.S. Ahn, Mol. Catal. 437 (2017) 73–79.
[11] M.S. Lohse, T. Bein, Adv. Funct. Mater. 28 (2018) 1705553.
[12] V.S. Vyas, F. Haase, L. Stegbauer, G.K. Savasci, F. Podjaski, C. Ochsenfeld, B.V. Lotsch, Nature Commun. 6 (2015) 8508.
[13] Y.L. Wan, Y.Z. Lei, G.S. Lan, D.F. Liu, G.X. Li, R.X. Bai, Appl. Catal. A Gen. 562 (2018) 267–275.
[14] J.X. Jiang, A. Trewin, D.J. Adams, A.I. Cooper, Chem. Sci. 2 (2011) 1777–1781.
[15] V. Sadhasivam, R. Balasaravanan, C. Chithiraikumar, A. Siva, ChemCatChem 10 (2018) 3833–3844.
[16] L.Y. Chen, R. Luque, Y.W. Li, Dalton Trans. 47 (2018) 3663–3668.
[17] D.N. Bunck, W.R. Dichtel, Chem. Commun. 49 (2013) 2457–2459.
[18] X.K. Chen, W.L. Wang, H.J. Zhu, W.S. Yang, Y.J. Ding, Mol. Catal. 456 (2018) 49–56.
[19] M. Bhadra, H.S. Sasmal, A. Basu, S.P. Midya, S. Kandambeth, P. Pachfule, E. Balaraman, R. Banerjee, ACS Appl. Mater. Interfaces 9 (2017) 13785–13792.
[20] S.Y. Chen, T. Yokoi, C.Y. Tang, L.Y. Jang, T. Tatsumi, J.C.C. Chan, S.F. Cheng, Green Chem. 13 (2011) 2920–2930.
[21] D. Chandra, B.K. Jena, C.R. Raj, A. Bhaumik, Chem. Mater. 19 (2007) 6290–6296.
[22] S.M.J. Rogge, A. Bavykina, J. Hajek, H. Garcia, A.I.O. Suarez, A.S. Escribano, A. Vimont, G. Clet, P. Bazin, F. Kapteijn, M. Daturi, E.V.R. Fernandez, F.X.L. Xamena, V. VanSpeybroeck, J. Gascon, Chem. Soc. Rev. 46 (2017) 3134–3184.
[23] V. Pascanu, P.R. Hansen, A.B. Gomez, C. Ayats, A.E. Platero-Prats, M.J. Johansson, M.A. Pericas, B. Martin-Matute, ChemSusChem 8 (2015) 123–130.
[24] M. Choi, D.H. Lee, K. Na, B.W. Yu, R. Ryoo, Angew. Chem. Int. Ed. 48 (2009) 3673–3676.
[25] Y. Zhou, H.C. Zeng, Chem. Mater. 29 (2018) 6076–6086.
[26] H. Pellissier, Adv. Synth. Catal. 357 (2017) 2745–2780.
[27] I.P. Beletskaya, F. Alonso, V. Tyurin, Coord. Chem. Rev. 385 (2019) 137–173.
[28] S. Bhunia, S.K. Das, R. Jana, S.C. Peter, S. Bhattacharya, M. Addicoat, A. Bhaumik, A. Pradhan, ACS Appl. Mater. Interfaces 9 (2017) 23843–23851.
[29] E. Berardo, R.L. Greenaway, L. Turcani, B.M. Alston, M.J. Bennison, M. Miklitz, R. Clowes, M.E. Briggs, A.I. Cooper, K.E. Jelfs, Nanoscale 10 (2018) 22381–22388.
[30] M.K. Bhunia, S.K. Das, P. Pachfule, R. Banerjee, A. Bhaumik, Dalton Trans. 41 (2012) 1304–1311.
[31] D. Hirasawa, Y. Watanabe, T. Yamahara, K. Tanaka, K. Sato, T. Yamagishi, Mol. Catal. 452 (2018) 184–191.
[32] F. Alonso, M. Yus, ACS Catal. 2 (2012) 1441–1451.
[33] S. Venkatraman, T. Huang, Chao-Jun Li, Adv. Synth.Catal. 344 (2002) 399–405.
[34] S.V. Damle, D. Seomoon, P.H. Lee, J. Org. Chem. 68 (2003) 7085–7087.
[35] L. Wang, Y. Zhang, L. Liu, Y. Wang, J. Org. Chem. 71 (2006) 1284–1287.
[36] Y. Li, J. Jin, W.X. Qian, W.L. Bao, Org. Biom Chem. 8 (2010) 326–330.
[37] B. Cirera, Y.Q. Zhang, S. Klyatskaya, M. Ruben, F. Klappenberger, J.V. Barth, ChemCatChem 5 (2013) 3281–3288.
[38] E. Rozhko, A. Bavykina, D. Osadchii, M. Makkee, J. Gascon, J. Catal. 345 (2017) 270–280.
[39] F. Strieth-Kalthoff, A.R. Longstreet, J.M. Weber, T.F. Jamison, ChemCatChem 10 (2018) 2873–2877.
[40] W. Liu, A. Lei, Tetrahedron Lett. 49 (2008) 610–613.
[41] L. Wang, W. Zhang, D.S. Su, X. Meng, F.S. Xiao, Chem. Commun. 48 (2012) 5476.
[42] R.N. Dhital, A. Murugadoss, H. Sakurai, Chem. Asian J. 7 (2012) 55.
[43] B.C. Ranu, T. Mandal, J. Org. Chem. 69 (2004) 5793–5795.
[44] K.K. Krishnan, S.M. Ujwaldev, A.P. Thankachan, N.A. Harry, G. Anilkumar, Mol. Catal. 440 (2017) 140–147.
[45] F. Nouri, S. Rostamizadeh, M. Azad, Mol. Catal. 443 (2017) 286–293.
[46] Y. Liu, D. Zhang, S. Xiao, Y. Qi, S. Liu, Asian J. Org. Chem. 8 (2019) 858–862.
[47] G. Cheng, M. Luo, Eur. J. Org. Chem. 13 (2011) 2519–2523.
[48] O. M.Yaghi, A. U. Czaja, B. Wang, Z. Lu, US Pat.2012/0130113, 2012.
[49] P. Puthiaraj, P. Suresha, K. Pitchumani, Green Chem. 16 (2014) 2865–2875.
[50] C.K. Wu, M. Yin, S. O'Brien, J.T. Koberstein, Chem. Mater. 18 (2006) 6054–6058.
[51] A.B. Bodade, M.A. Taiwade, G.N. Chaudhari, J. Appl. Pharma. Res. 5 (2017) 30–39.
[52] Md.M. Islam, M. Halder, A.S. Roy, Sk.M. Islam, ACS Omega 2 (2017) 8600–8609.
[53] I. Miletto, G. Paul, S. Chapman, G. Gatti, L. Marchese, R. Raja, E. Gianotti, Chem. Eur. J. 23 (2017) 9952–9961.
[54] A.K. Patra, S.K. Das, A. Bhaumik, J. Mater. Chem. 21 (2011) 3925–3930.
[55] S.K. Das, K. Bhunia, A. Mallick, A. Pradhan, D. Pradhan, A. Bhaumik, Microporous`Mesoporous Mater. 266 (2018) 109–116.
[56] K. Borgohain, J.B. Singh, M.V. Rama Rao, T. Shripathi, S. Mahamuni, Phys. Rev. B 61 (2000) 11093–11096.
[57] T. Premkumar, K.E. Geckeler, Small 2 (2006) 616–620.
[58] A. Jain, K.B. Pandeya, Trans. Metal Chem. 19 (1994) 81–83.
[59] S.S.E. Ghodsinia, B. Akhlaghinia, Green Chem. 21 (2019) 3029–3049.
[60] C.A. Martínez, K.V.T. Nguyen, F.S. Ameer, J.N. Ankerand, J.L. Brumaghim, Nanotoxicology 11 (2017) 278–288.
[61] G. Cheng, M. Luo, Eur. J. Org. Chem. (2011) 2519–2523.
[62] B. Kaboudin, Y. Abedi, T. Yokomatsu, Eur. J. Org. Chem. (2011) 6656–6662.
[63] P. Puthiaraj, P. Suresha, K. Pitchumani, Green Chem. 16 (2014) 2865–2875.